Oncology Research, Vol. 28, pp. 177–189
Printed in the USA.

0965-0407/20 $90.00 + .00
DOI: https://doi.org/10.3727/096504019X15746768080428
E-ISSN 1555-3906
www.cognizantcommunication.com

IOX-101 Reverses Drug Resistance Through Suppression of Akt/mTOR/NF-κB Signaling in Cancer Stem Cell-Like, Sphere-Forming NSCLC Cell

Majed Al Fayi,*† Ahmad Alamri,* and Prasanna Rajagopalan*†

*Department of Clinical Laboratory Sciences, College of Applied Medical Sciences, King Khalid University, Abha, Saudi Arabia
†Central Research Laboratory, College of Applied Medical Sciences, King Khalid University, Abha, Saudi Arabia

Drug discovery research to fight lung cancer is incessantly challenged by drug resistance. In this study, we used drug-resistant lung cancer stem like cells (A549-CS) to compare the efficacy of standard drugs like cisplatin (DDP) and gemcitabine (GEM) with a novel arylidene derivative IOX-101. A549-CS was derived from regular A549 cells by growing in special media. Resistance proteins were detected using Western blotting. Cell proliferations were assessed by MTT assay. Cytokine release was enumerated using enzyme-linked immunosorbent assay. The effect of drugs on apoptosis and cell cycle was studied with flow cytometry protocols. Apoptosis-related proteins, caspases, and other signaling protein expressions like Akt and mammalian target of rapamycin (mTOR) were assessed by Western blotting. Expression of CD133 and nuclear factor B (NF- B) phosphorylation was assessed using flow cytometry. A549-CS showed significant increase in CD133 expression in comparison with A549 cells. Expression of resistance markers like MDR-1, lung resistance protein (LRP), and GST-II were detected in A549-CS. While DDP and GEM had relatively lower efficacy in A549-CS, IOX-101 inhibited the proliferation of both A549 and A549-CS with GI_{50} values of 268 and 296.5 nM, respectively. IOX-101 increased the sub-G_0 phase in the cell cycle of A549-CS and increased the percentage of apoptotic cells. Western blot analysis revealed activation of caspases, Bax, and reduction in Bcl-2 levels. Further mechanistic investigation revealed IOX-101 to deactivate Akt, mTOR, and NF- B signaling in A549-CS cells. Additionally, IOX-101 treatment to A549-CS also reversed MDR-1 and LRP expressions. Collectively, our results demonstrate efficacy of IOX-101 in A549-CS, which was resistant against the tested standard drugs. The activity was mediated by suppressing Akt/mTOR/NF- B signaling.

Key words: A549; A549-CS; Akt; CD133; Drug resistance; GST-II; Lung resistance protein (LRP); Lung cancer; Multidrug resistance gene (MDR-1); mTOR; NF-κB; Stem-like cells

INTRODUCTION

Drug resistance is a condition where the cancer cells, viruses, or bacteria do not/weakly respond to medications, ultimately resulting in ineffective treatments. Multidrug resistance (MDR) is described as decreased bioactivity for an array of drugs used in treatments and is considered a growing worldwide public health threat. Cancer drugs generally are metabolically activated to execute their efficacy in cancer cells, where any alteration of this activation could end up in resistance. Occurrence of resistance in cancer cells could be due to more than one factor[1]. A drug's efficacy preliminarily relies on its molecular target, and any alterations to these targets could result in drug resistance[2]. Modification in key enzyme expressions at the target end may be another reason[3]. Studies reveal that cancer drug resistance may involve drug accumulation reduction as a reason of efflux[4]. It has been reported that drug resistance can arise during repairing mechanisms in DNA posttreatment of DNA-damaging agents like cisplatin (DDP)[5]. Epithelial–mesenchymal transition (EMT) or cell death inhibition has accounted for drug resistance in some cancer types[6]. Interestingly, modification of epigenetics is also identified as a major reason for resistance in a few cancer treatments[7]. On any of the above cases, overcoming drug resistance in cancer treatment is a real challenge, and the search for different options to overcome drug resistance remains incessant.

Lung cancer is the leading cause of cancer-related deaths worldwide, where non-small cell lung carcinoma (NSCLC) is the most common type of lung cancer, accounting for nearly 80% of lung cancer cases[8]. Chemotherapy

Address correspondence to Prasanna Rajagopalan, Department of Clinical Laboratory Sciences, Room No-131, Building C, College of Applied Medical Sciences, King Khalid University, Abha, Asir, Saudi Arabia. Tel: +966540924232; E-mail: rajagopalan@kku.edu.sa *or* prachu.rg@gmail.com

remains the primary choice for treating NSCLC patients to reverse clinical symptoms and develop quality of life. Although initially patients respond to chemotherapeutics, eventually most lung cancer types develop drug resistance, resulting in a setback to the treatment. DDP and gemcitabine (GEM) are widely used as chemotherapeutics in the treatment of lung cancer due to their potent antitumor activities[9]. However, efficacy of treatment in lung cancer is often limited by the occurrence of innate and acquired drug resistance[10]. Combination chemotherapy of drugs like DDP, docetaxel, GEM, and paclitaxel remains as a choice to overcome drug resistance in lung cancer[11]. However, side effects like nephrotoxicity, nausea, and vomiting are often observed during these combination therapies[11]. Therefore, identification of new anticancer agents is needed for a more effective treatment for NSCLC patients. IOX-101 is a novel arylidene derivative that has potent anticancer effects. We have evaluated this molecule against leukemic cell lines and proven it to work efficiently against acute myeloid leukemia (AML) cells by inhibiting the Akt enzyme and causing nuclear fragmentation[12].

It has been proven that when NSCLC cells were enriched for stem-like cells by using a special growth medium, they express numerous stem cell markers, which results in them having morphological and physiological characteristics with drug-resistant properties[13]. In the current study, this model was used to evaluate the anticancer properties of DDP, GEM, and IOX-101 in drug-resistant lung cancer cells.

MATERIALS AND METHODS

Materials

All chemicals and reagents were purchased from Sigma-Aldrich (St. Louis, MO, USA) unless otherwise indicated. A549, HEL299, and HUV-EC-C [human umbilical cord endothelial cells (HUVEC)] cell lines were purchased from the American Type Culture Collection (ATCC; Manassas, VA, USA). Annexin-V kit, anti-CD133-fluorescein isothiocyanate (FITC) antibody, and enzyme-linked immunosorbent assay (ELISA) cytokine kits were obtained from e-Bioscience (San Diego, CA, USA). Recombinant human hepatocyte growth factor (HGF), transendothelial migration assay kit, and Guava cell cycle reagent were obtained from Millipore Corp. (Boston, MA, USA). All antibodies for Western blotting, unless specified, were purchased from Abcam (Cambridge, UK). Caspases 3 and 9, Bcl-2, Bax, and actin antibodies were purchased from Santa Cruz Biotechnology (Santa Cruz, CA, USA). Phospho-nuclear factor B (NF- B) p65 (S529) phycoerythrin (PE) antibodies were from Thermo Scientific (Waltham, MA, USA).

Cell Culture

A549 cells were grown in Dulbecco's modified Eagle's medium (DMEM) (ATCC) medium, and HEL299 cells were cultured on EMEM (ATCC) medium. HUVECs were maintained in F12K full growth medium, with 0.1 mg/ml heparin, 0.05 mg/ml endothelial cell growth supplement (ECGS), and adjusted to a final concentration of 10% fetal bovine serum (FBS). All complete growth medium contained 10% FBS, 100 U/ml of penicillin, and 100 U/ml streptomycin. Cells (passages 3–12) were maintained in a humidified atmosphere of 5% CO_2 incubator at 37ºC until the confluence stage was attained. The medium was replaced every other day, and the maintenance was strictly in accordance with standard methods. Assays were performed when the cell were 70% confluent.

A549-CS Cultures

A549-CS cells were cultured in modified DMEM medium, henceforth referred to as CS-medium containing B27 (1×), recombinant human epidermal growth factor (rhEGF; 20 ng/ml), basic fibroblast growth factor (bFGF; 20 ng/ml), and insulin (4 U/L). A549-CS cells were prepared as described elsewhere[13]. Briefly, 1×10^3 A549 cells were seeded in six-well plates and cultured in CS-medium for 2–3 weeks until floating small spheres were observed. When the small primary spheres reached 100–200 cells/spheres, they were separated as single cells and recultured in CS-medium for the next 2 weeks to form larger secondary spheres. These secondary spheres, hereafter referred to as A549-CS, were characterized and used in the experiments.

Cell Viability Assay

Viability assays were performed as described by Mosmann[14] with minor modifications. Briefly, 100 µl of growth media containing 5,000 cells was plated in triplicates in a 96-well plate. Cells were added with 50 µl of DDP/GEM/IOX-101 to obtain the desired final concentration along with a dimethyl sulfoxide (DMSO) blank and incubated at 37°C and 5% CO_2 for 72 h. The cell medium was replaced with 100 µl of MTT (1 mg/ml) and incubated for 3.5 h. Media were aspirated and MTT was dissolved in 200 µl of DMSO, and absorbance was read at 560 nm with reference at 640 nm. Percentage inhibition was calculated after subtracting day 0 MTT reads. Results were analyzed using GraphPad Prism software (Version 5.02; La Jolla, CA, USA).

Annexin V Assay

The Annexin-V assay kit from e-Biosciences was used to analyze apoptosis. Cells (0.5×10^6) were treated with the respective concentrations of DDP/GEM/IOX-101 and incubated in a CO_2 incubator for 48 h. Cells were stained with 0.25 µg/ml annexin V reagent and incubated at room temperature for 15 min in the dark. After a wash with phosphate-buffered saline (PBS), cells were resuspended in buffer containing 0.5 µg/ml propidium iodide and

acquired on a Guava easyCyte™ flow cytometer. Data analysis was performed using the InCyte software from Millipore.

Cell Cycle Analysis

A549 cells and A549-CS were incubated with DDP/GEM/IOX-101 at the desired concentrations for 48 h at 37°C and fixed with 70% ethanol until analysis. Further, cell cycle reagent from Millipore was used to stain the cells, and events were acquired on a Guava easyCyte™ flow cytometer. ExpressPro software from Millipore was used for the analysis.

Transendothelial Cell Migration Assay

The assay was carried out with QCM™ Tumor Cell Transendothelial Migration Assay colorimetric kit from Millipore as per the manufacturer's instructions. Briefly, 1×10^5 HUVECs were grown on migration inserts until confluent. A549-CS (1×10^5) were starved overnight in a serum-free media and replaced with the media in the inserts. The inserts were further transferred to new wells with serum-free tumor cell growth media containing ±25 ng/ml HGF at final concentration. Postincubation in a CO_2 incubator for 12 h, the media were removed from the inserts, stained, and eluted. Eluent was transferred to a 96-well stain quantification plate, and absorbance was read at 540–570 nm.

Cytokine Estimations by ELISA

Effects of IOX-101 on the inflammatory mediator cytokine release from A549-CS were analyzed by ELISA. A549-CS were plated in six-well plates and were incubated with different concentrations of IOX-101 for 1 h, followed by 10 mg/ml lipopolysaccharide (LPS) induction for 24 h. Collected supernatants were stored at −80°C until analysis. Levels of tumor necrosis factor- (TNF-), interleukin-6 (IL-6), and IL-8 were assessed by kit protocols as per the manufacturer's instructions. The color that developed was measured for absorbance at 450 nM.

Western Blotting

Protein lysates from A549 cells and A549-CS from healthy cultures were used for basal level detection of MDR-1, lung resistance protein (LRP), and GST-II proteins. For estimations using treatments, A549-CS were pretreated with desired concentrations of IOX-101 along with DMSO blanks and incubated for 24 h in 37°C in a CO_2 incubator. All cells were lysed in lysis buffer, and total protein concentration was estimated by Coomassie Plus Protein Assay Reagent Kit (Pierce, Rockford, IL, USA). Protein (20–40 µg) from the cell lysate was separated with sodium dodecyl sulfate-polyacrylamide gel electrophoresis (SDS-PAGE) and then transferred to nitrocellulose membrane, probed with respective primary antibodies. Horseradish peroxidase (HRP) secondary antibodies were added, and the membrane was stripped after a 30-min incubation. Bands were quantified using ImageJ (Ver. 1.46, National Institutes of Health) and normalized to -actin (1:5,000).

Flow Cytometry

Detection of CD133 and phosphorylated NF- B was performed by flow cytometry as described elsewhere[15] with minor modifications. Briefly, 0.5×10^6 cells were plated in 2 ml of cell growth media in six-well plates and incubated overnight at 37°C and 5% CO_2. Healthy, untreated A549 cells/A549-CS were used to detect CD133. For NF- B detection, A549-CS were treated with IOX-101 for 24 h in a regular cell incubator. Cells were stained for 20 min in the dark with anti-CD133 FITC or phospho-NF- B p65 PE antibodies in intracellular fixation and permeabilization buffer reagent (Thermo Scientific). After a couple of washes with washing buffer, the cells were resuspended in PBS and 5,000 events were acquired in a Guava easyCyte™ flow cytometer. Cells were gated for CD133 or phosphorylated NF- B-positive events and analyzed using ExpressPro software from Millipore.

Statistical Analysis

Each experiment was carried out at least in triplicate, and results were expressed as mean ± standard deviation. Statistical analyses were performed using GraphPad Prism 5.02. GI_{50} values were calculated using a nonlinear regression fit model with variable slope and plotted accordingly. Differences between two groups were analyzed using two-tailed Student's *t*-test, whereas those between three or more variants were analyzed using one-way analysis of variance (ANOVA) comparisons. Differences with values of $p < 0.001$ and $p < 0.05$ were considered statistically significant.

RESULTS

A549 Sphere-Forming Cancer Cells (A549-CS) Express Morphological Modification and Phenotype Markers Typical to Drug Resistance Cells

A549-CS showed distinct characteristics when compared with regular A549 cells. A549-CS lost epithelial morphology, adhesive properties, and formed floating clusters. Small clusters/primary spheres (Fig. 1A-a) were observed after the first week. Big clusters/secondary spheres (Fig. 1A-b) were cultured from single cells of the primary spheres using CS medium. After preparing single-cell suspensions from A549-CS and A549 cells, CD133 expression was assessed by flow cytometry. A549-CS showed a clear right shift in the fluorescence peak indicative of CD133-positive population (Fig. 1 B-a, b). A549

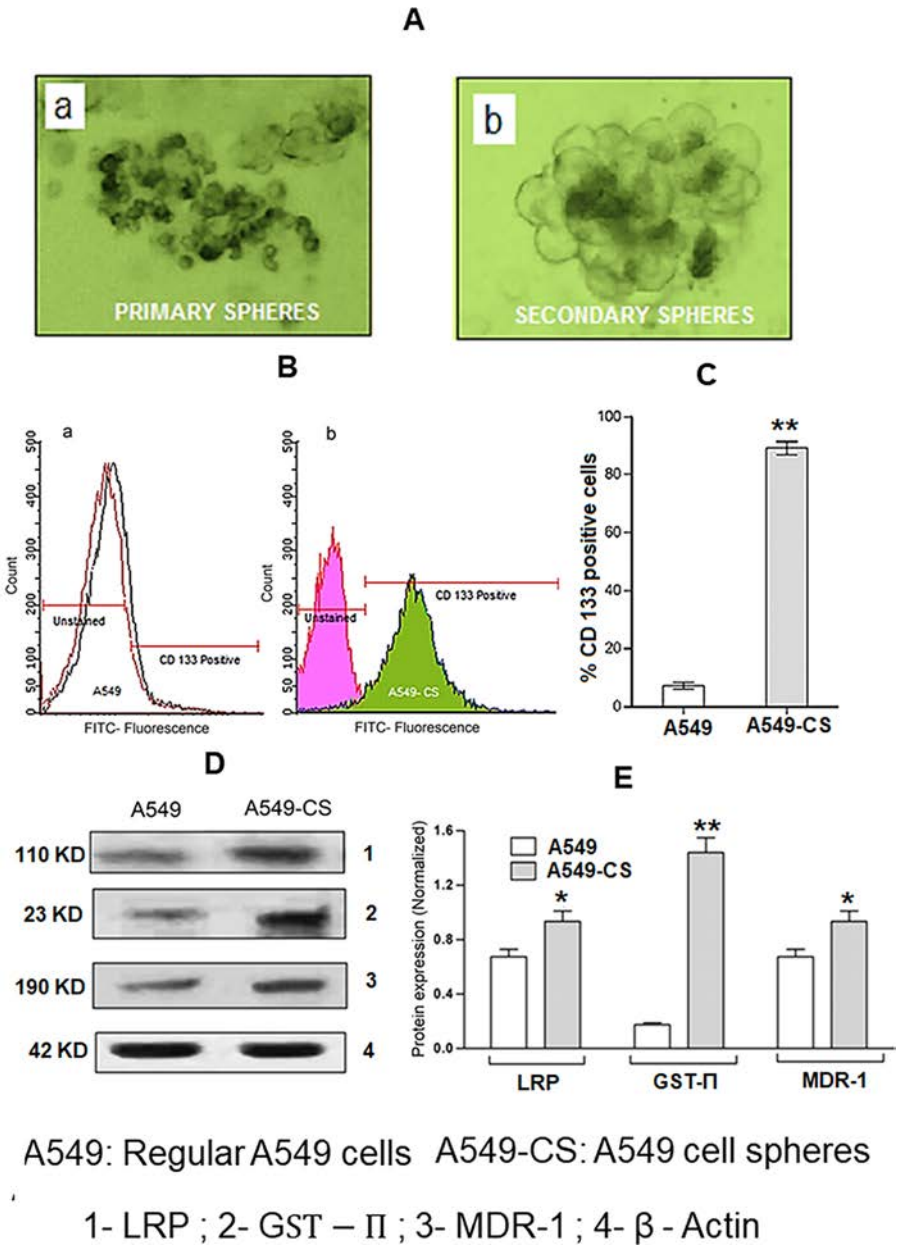

Figure 1. Characterization of A549-CS in comparison with normal A549 cells. (A) Morphological characterization of A549-CS cells. Primary spheres (a) formed in the medium and secondary spheres (b) were derivatives of parental cells. Magnification: 200×. (B) CD133 marker detection in A549 and A549-CS cells by flow cytometry. Representative histograms from three individual experiments are shown. (C) Percentage of the CD133-positive population in A549-CS compared with A549 cells. Results were expressed as mean ± standard deviation (SD) from three separate experiments. $^{**}p < 0.001$. (D) Physiological characterization of A549-CS compared with A549 cells. Enhanced expression of lung resistance protein (LRP), GST-II, and MDR-1 proteins was observed in A549-CS detected by Western blotting. Representative bands from different repeats of experiments are shown. (E) Quantified representations of resistance proteins from Western blot. Results were expressed as mean ± SD from three separate experiments. $^{*}p < 0.05$, $^{**}p < 0.001$.

cells had 7.35% CD133-positive cells, while 89.11% of A549-CS were positive for CD133 (Fig. 1C). When evaluated for the expression of drug resistance markers like LRP, GST-II, and MDR-1 (Fig. 1D), all these proteins were markedly increased in A549-CS (Fig. 1E).

Drug Resistance Characteristics of A549-CS

With the observed expression of drug resistance markers in A549, we next evaluated the efficacy of two anticancer drugs DDP and GEM in A549-CS in comparison with the regular A549 cells. DDP inhibited the proliferation of

A549 and A549-CS with GI_{50} values of 4.86 and 52.80 µM (Fig. 2A-a). The effect of GEM in inhibiting A549 proliferation was relatively higher with GI_{50} value of 8.88 µM when compared with A549-CS, which showed a GI_{50} value of 24.65 µM (Fig. 2B-a). Reductions of ninefold potency for DDP (Fig. 2A-b) and threefold potency for GEM (Fig. 2B-b) were observed in A549-CS compared with A549 cells. The annexin V assay revealed a clear increase in early and late phase apoptotic cells in A549 cells treated with DDP and GEM (Fig. 3A-a–c, B), whereas apoptosis was relatively less in A549-CS treatments (Fig. 3A-d–f, B). Cell cycle analysis of A549 cells and A549-CS showed different characteristics. Treatment of A549 cells with DDP and GEM increased the G_0/G_1 phase population to 67.12% and 71.23%, respectively, compared to untreated control, which had 55.13% in the G_0/G_1 phase (Fig. 4a–c). While A549 control cells showed a normal cell cycle distribution (Fig. 4a), A549-CS control cells showed increased accumulation in the G_2/M phase (Fig. 4d). DDP and GEM treatments to A549-CS did not alter the cell cycle when compared with control (Fig. 4d–f).

IOX-101 Exhibits Efficacy in A549-CS by Cell Cycle Changes and Apoptosis Induction

Next, we analyzed the effect of IOX-101 in A549 and A549-CS proliferations. IOX-101 was effective in stopping the proliferations of both these cell types at GI_{50} values of 268 and 296.5 nM for A549 and A549-CS, respectively (Fig. 5A-a). The compound did not affect the proliferation of noncancerous, normal lung fibroblast cells (HEL299) at near concentrations of cancer cell inhibitions (Fig. 5A-a), showing nearly sixfold less potency compared with A549 and A549-CS cells (Fig. 5A-b). Both early and late phase apoptosis were detected in A549-CS when treated with 300 nM IOX-101 (Fig. 5B-a, b). The appearance of a hypodiploid peak in the cell cycle was observed in A549-CS cancer cells after IOX-101 treatment (Fig. 5C). An increase in the percentage of sub-G_0 phase cells from 3.32% to 24.873% was observed when compared to control (Fig. 5C). IOX-101

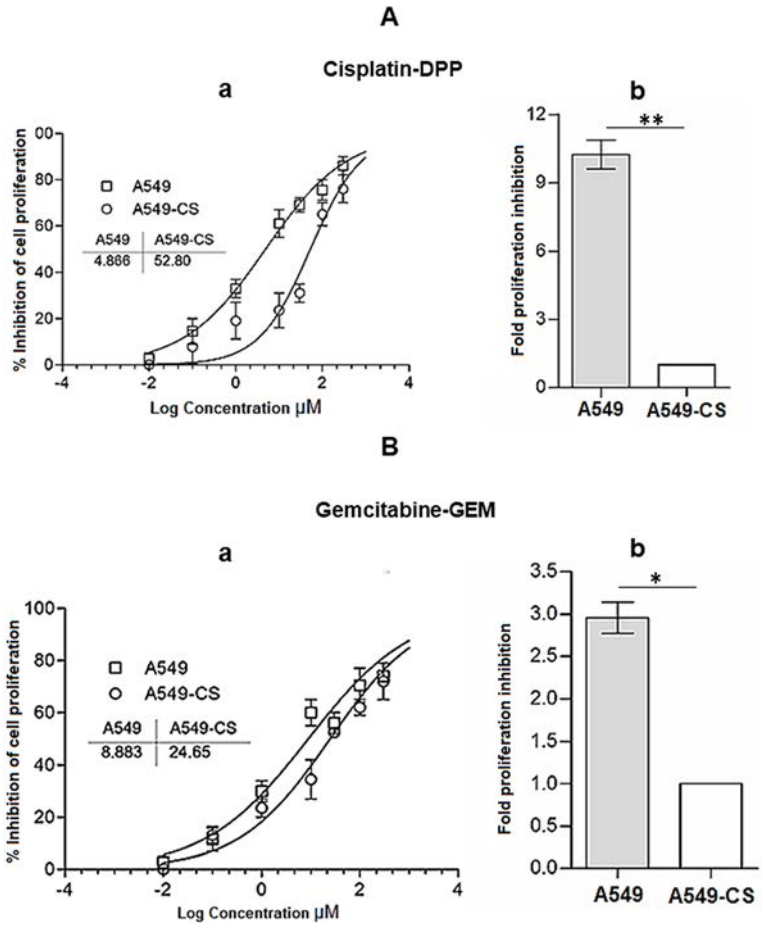

Figure 2. Anticancer drug sensitivity in A549 cells and A549-CS evaluated by MTT assay with (A-a) cisplatin (DDP) and (B-a) gemcitabine (GEM) treatments for 72 h. GI_{50} from three individual experiments performed in triplicates are shown. Histograms show fold difference in cell proliferation inhibition by DDP (A-b) and GEM (B-b). *$p < 0.05$, **$p < 0.001$.

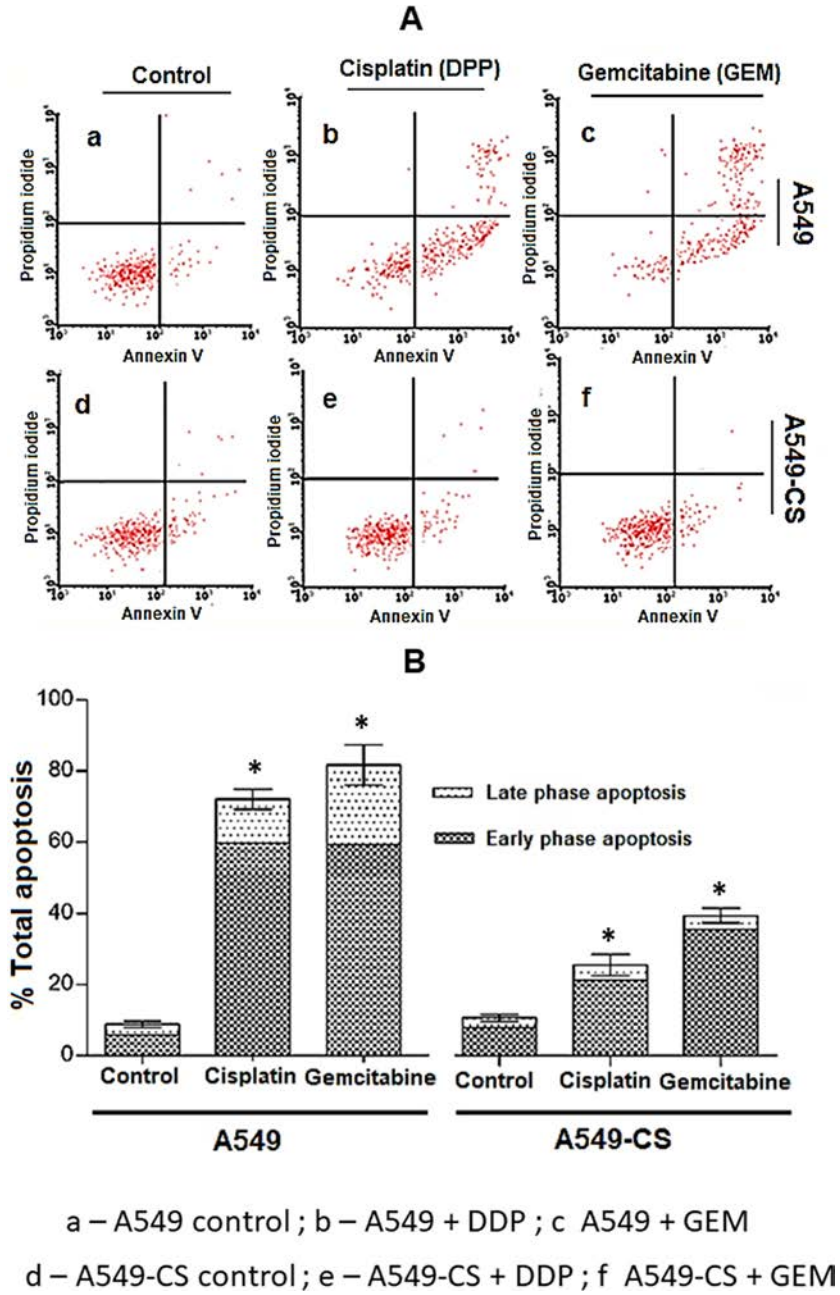

Figure 3. Apoptosis resistance properties of A549-CS with standard drugs in comparison with regular A549 cells. (A) Quadri plot graphs represent apoptosis induction by DDP and GEM in A549 and A549-CS treated with respective GI_{50} doses. Cells were stained with annexin V–fluorescein isothiocyanate (FITC) and propidium iodide and analyzed by flow cytometer for early and late phase apoptosis. Representative quadri plots from three individual experiments are shown. (B) Graphical representation of early and late phase apoptosis from quadri plots. Results were expressed as mean ± SD. $*p < 0.05$.

treatment also decreased G_2/M phase A549-CS from 40.13% to 26.23% when compared to untreated control (Fig. 5C).

Cancer Cell Migration Inhibition and Attenuation of Cytokine Expressions by IOX-101 in A549-CS

The effect of IOX-101 to inhibit cancer cell migration was analyzed using transendothelial cell migration assay under the influence of hepatocyte growth facto (HGF) as chemoattractant. IOX-101 dose-dependently inhibited the migration of A549-CS across HUVEC cell membrane (Fig. 6A). IOX-101 also inhibited the release of TNF- (Fig. 6B), IL-6 (Fig. 6C), and IL-8 (Fig. 6D) by A549-CS in the medium when induced with LPS. The effect of IOX-101 inhibition of these cytokines was found to be

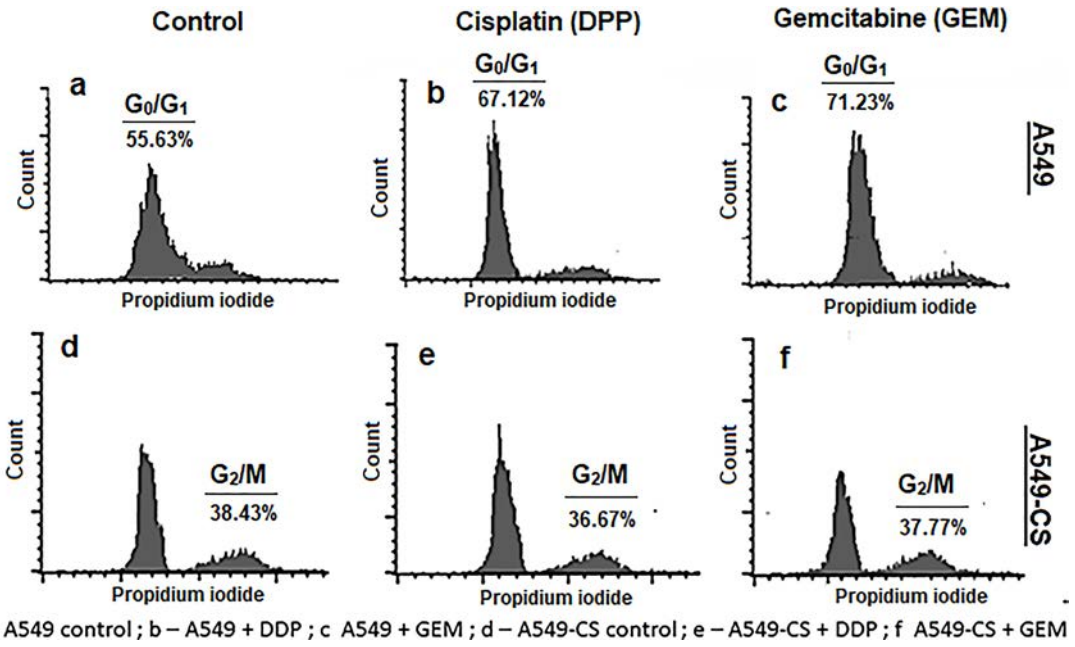

Figure 4. Flow cytometric analysis of cell cycle changes in A549 and A549-CS cells after respective GI_{50} dose treatments with DDP or GEM for 48 h. Numbers in the histogram graphs indicate percentage cell population in the G_0/G_1 or G_2/M phase of the cell cycle. Data shown represent graphs from three independent experiments.

dose-dependently reduced with the increase in concentrations of IOX-101.

IOX-101 Reverses MDR by Promoting Apoptosis-Related Proteins Through the Akt/Mammalian Target of Rapamycin (mTOR)/NF-κB Pathway

To assess the effects of apoptosis induction by IOX-101 in A549-CS, we evaluated activation of caspases and levels of apoptosis-associated proteins (Fig. 7A-a). Dose-dependent increase in both caspases 3 and 9 was observed with IOX-101 treatments (Fig. 7A-b). IOX-101 decreased antiapoptotic Bcl-2 expression and increased proapoptotic Bax expression in A549-CS (Fig. 7A-a, b). Bcl-2/Bax ratio significantly reduced with increasing concentrations of IOX-101 treatments (Fig. 7D). We studied the effects of IOX-101 treatment on Akt pathway proteins. Phosphorylation of Akt and its downstream target mTOR was dose dependently reduced in A549-CS, while no changes were observed in total Akt and total mTOR expressions in these cells (Fig. 7B-a, b). The levels of resistance of protein expressions after IOX-101 treatment were also evaluated. Dose-dependent reduction in MDR-1 and LRP levels was observed with the compound treatment in A549-CS (Fig. 7C-a, b). Inhibition of NF- B/p65, the downstream effector protein of Akt/mTOR, was determined by flow cytometry. We used the higher concentration of 600 nM IOX-101 to check the best inhibition efficacy of the molecule in the tested range. Treatment with IOX-101 markedly reduced the percentage of NF- B/p65-positive cells to 33.23% from 77.13% in comparison with the untreated control A549-CS (Fig. 8).

DISCUSSION

MDR in cancer treatments is a continuous challenge faced by clinicians and researchers globally. While several in vitro models are used to test drug resistance, frequent protocols follow treating cancer cells with drugs for longer periods and creating a drug efflux from cells to make them resistant[16]. However, developing a chemotherapy drug-resistant cancer cell line is a long-established approach, and success rate chiefly depends on the parental cell line, treatment dose, and time periods[17]. Cancer stem cells (CSCs) are believed to play multiple roles in tumorigenesis, which are not limited to the initiation, development, and recurrence of tumors[18]. There is a considerable literature evidence that CSCs derived from glioma, leukemia (Fuchs D), hepatocellular carcinoma[19], prostate[20], thyroid[21], and ovarian carcinoma[22] exhibit features of drug resistance. We used A549 cells to create stem cell-like, sphere-forming cells (A549-CS) as described elsewhere[23]. Morphology of these spheres was very similar to the established procedure[24]. CD133 is not only considered as a stem cell marker but is also proven to be expressed in cancer-resistant cells[25]. CD133 expression in A549-CS therefore indicated stem cell likeliness and drug resistance property in these spheres. Expression of drug resistance proteins like MDR-1, LRP,

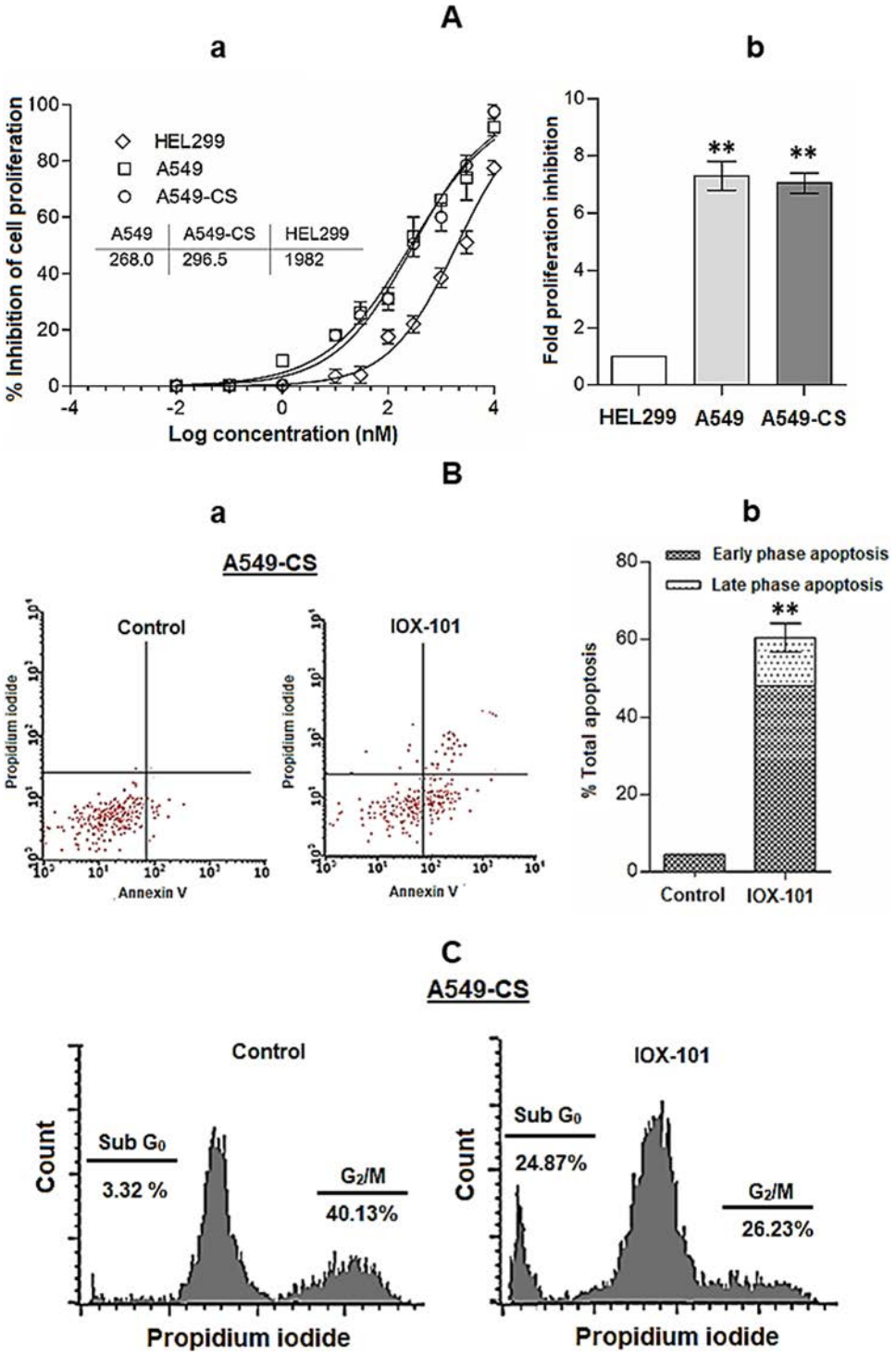

Figure 5. Anticancer efficacy of IOX-101 in normal lung (HEL299), regular lung cancer (A549), and resistant lung cancer (A549-CS) cells. (A-a) GI_{50} values for IOX-101 in A549-CS, A549, and HEL299 cells. (A-b) Fold difference of proliferation inhibition by IOX-101 in all three cells. Results were expressed as mean ± SD. $^{**}p < 0.001$. (B-a) Quadri plot graphs showing apoptosis induction in A549-CS treated with 300 nM IOX-101 in comparison with untreated control. (B-b) Histograms represent early, late, and total apoptosis in A549-CS after IOX-101 treatment in comparison to untreated control. Results were expressed as mean ± SD. $^{**}p < 0.001$. (C) Cell cycle analyses of untreated and IOX-101-treated A549-CS by flow cytometry. Representative data from three different experiments are shown.

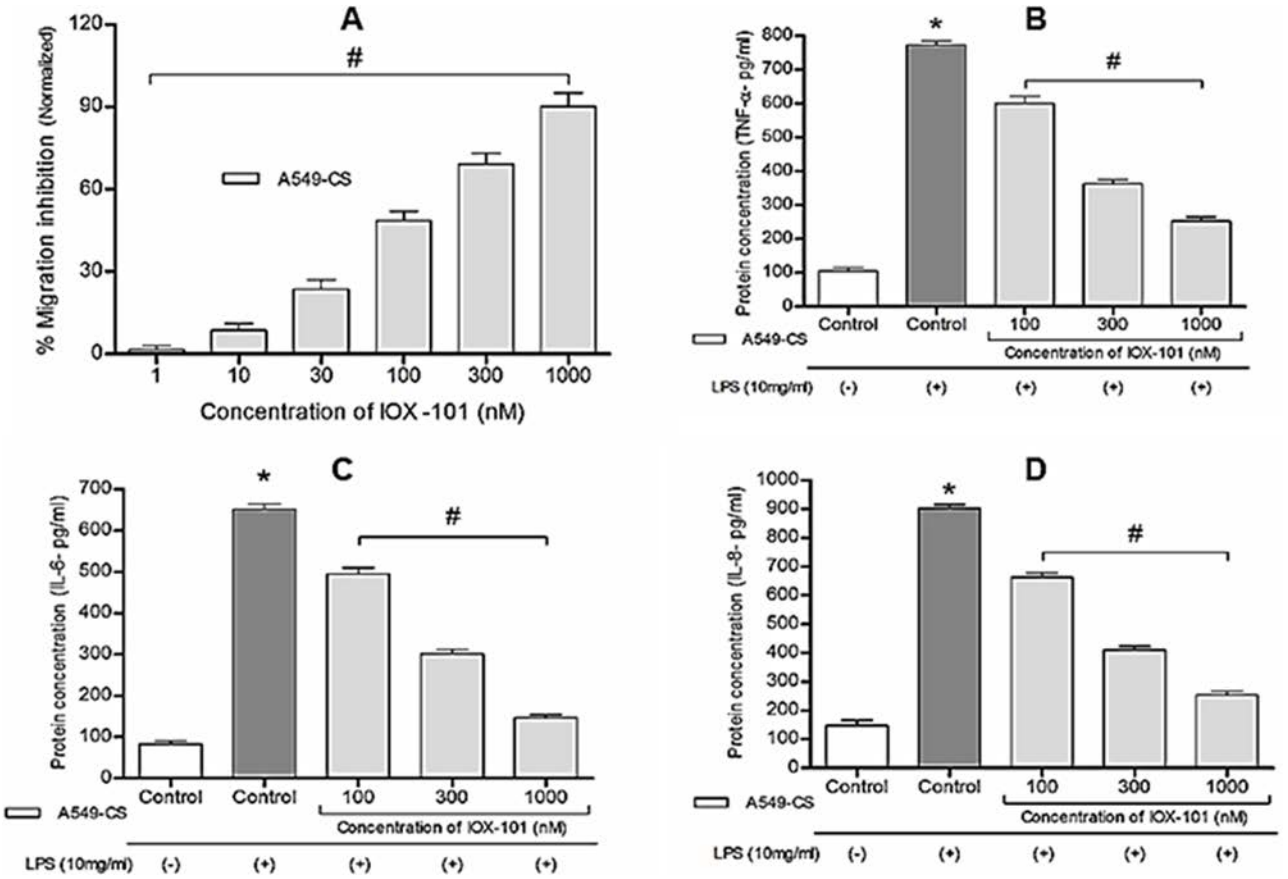

Figure 6. Cancer cell migration and cytokine release inhibition by IOX-101 in A549-CS. (A) Transendothelial migration assay showing the dose-dependent inhibition of A549-CS migration by IOX-101 across human umbilical cord endothelial cells (HUVECs) under the influence of hepatocyte growth factor (HGF) (25 ng/ml) at 12-h incubation time. IOX-101 pretreatment inhibited lipopolysaccharide (LPS) (10 µg/ml)-induced (B) tumor necrosis factor- (TNF-), (C) interleukin-6 (IL-6), and (D) IL-8 release in A549-CS detected by enzyme-linked immunosorbent assay (ELISA). *$p < 0.05$ when compared with uninduced control. #$p < 0.05$ within treatment doses.

and GST-II was relatively higher in A549-CS than in normal A549 cells, which further confirmed the drug resistance characteristics of these CSC spheres[26].

Our observations indicate A549-CS to exhibit significant resistance to DDP and GEM in controlling cell proliferations. These observations were in accordance with previous literature[27]. DDP and GEM induced early and late phase apoptosis in A549 cells[10], while apoptosis induction was significantly reduced by both drugs in A549-CS. These results were in line with the antiproliferative effects of DDP and GEM in A549 and A548-CS. As it is well proven that cell responses to chemotherapeutics rely on kinetics of cell cycle[28], we analyzed cell cycle changes in A549 and A549-CS with DDT and GEM treatments. Drug treatments increased the G_0/G_1 phase accumulations in A549 cells, which stood well with a previous report[29]. In contrast, A549-CS control cells exhibited relatively higher proportion of G_2/M phase cells when compared with A549 cells. This observation could be related with recent findings that cancer cells express longer G_2/M phase due to the DNA repair mechanisms, particularly when they are resistant to apoptosis[30]. Treatment with DDP and GEM did not alter the cell cycle of A459-CS, supporting the resistance characteristics of A549-CS acquired against these drugs. The resistant property of A549-CS against standard anticancer drugs therefore gains attention to use these cells as a robust model for screening drug resistance in lung cancer cells.

In the next phase of the study, we tested the efficacy of IOX-101 on proliferations of A549 cells and A549-CS. Our results clearly demonstrated the proliferation inhibitory efficacy of IOX-101 in normal and resistant lung cancer cells. Further, selectivity of the compound toward the cancer cells was evaluated by comparing with the noncancerous lung fibroblast cells. Observation of around eightfold potency in both A549 cells and A549-CS indicates the efficacy and selectivity of IOX-101 toward inhibition of cancer cell proliferation. This property can be

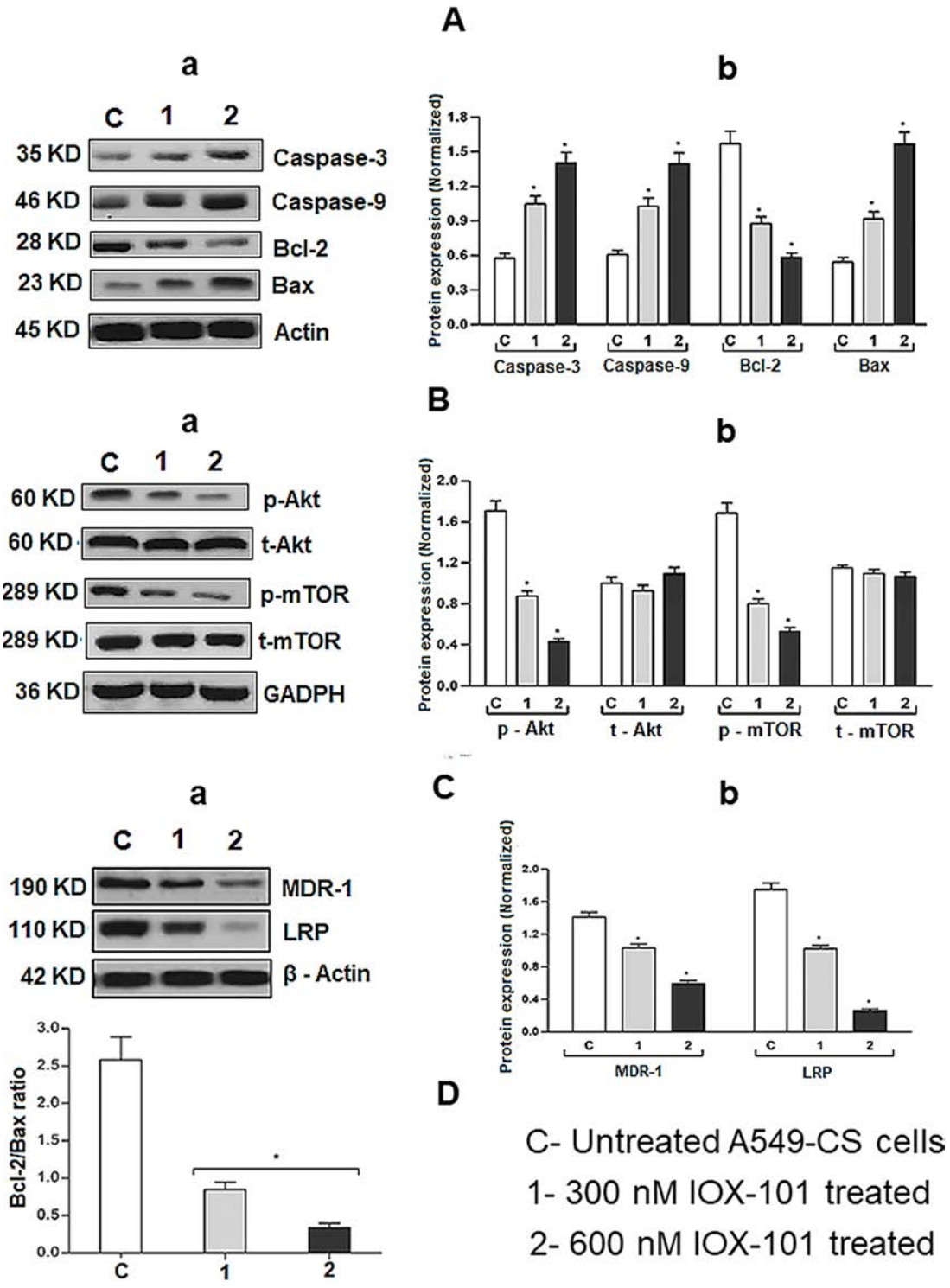

Figure 7. Regulation of apoptotic markers and Akt/mammalian target of rapamycin (mTOR) pathway by IOX-101 in A549-CS. (A-a) Western Blot of caspases, antiapoptotic, and proapoptotic markers after different doses of IOX-101 treatment in A549-CS for 48 h. (B-a) Dose-dependent inhibitory effect of IOX-101 on the phosphorylation of Akt and mTOR in A549-CS cell lines detected by Western Blotting. (C-a) Dose-dependent down regulation of MDR-1 and LRP expression in A549-CS by IOX-101 treatments. (A-b, B-b, C-b) Quantified representations of proteins from Western blot. Results were expressed as mean ± SD from three separate experiments. *$p < 0.05$. (D) Graphical representation for the effect of IOX-101 on Bcl-2/Bax ratio in A549-CS. All bands were quantified by densitometry using ImageJ (Ver. 1.46, National Institutes of Health). After normalizing to actin, results from the three individual experiments were expressed as mean ± SD and were plotted with GraphPad Prism 5. *$p < 0.05$.

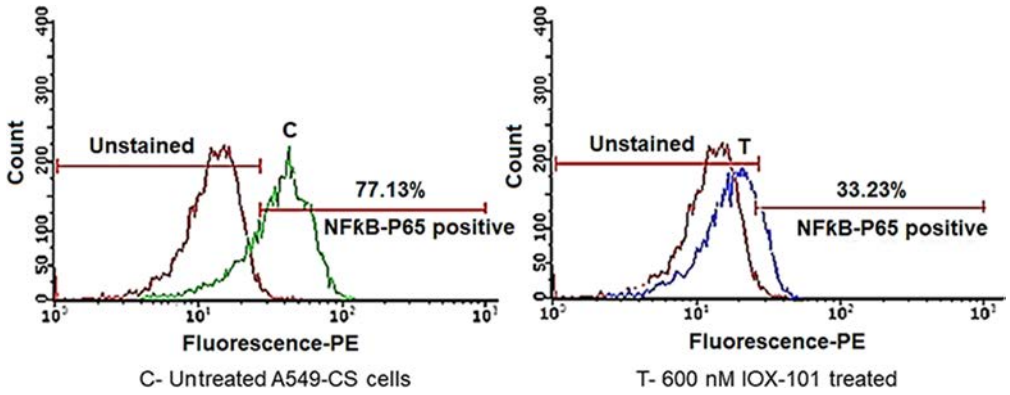

Figure 8. Attenuation of nuclear factor B (NF- B) expression by IOX-101 in A549-CS. Inhibitory effect of IOX-101 treatment on NF- B/p65 phosphorylation in A549-CS compared with untreated controls analyzed by flow cytometry. Representative graphs from three individual experiments are shown.

attributed to the reasonable in vitro therapeutic window by the compound. It is well proven that any compound with a potential to induce apoptosis can be considered as novel for cancer treatment. Annexin V binds with high affinity to phosphatidylserine of the mitochondrial membrane when exposed to apoptotic cell surface and differentiates healthy cells from apoptotic cells[31]. The occurrence of annexin V-positive cells after IOX-101 treatment confirmed the apoptotic induction by the compound in the resistant A549-CS cells. IOX-101 treatment reversed the G_2/M arrest in A549-CS, making them appear in the sub-G_0 region. Appearance of the hypodiploid peak in the cell cycle analysis indicates DNA damage induced by the compound in A549-CS[32]. It is shown that certain drugs cause DNA damage that results in stagnation of cells in the G_2/M phase prior to induction of apoptosis[33]. As the A549-CS cells were already stagnant in the G_2/M phase, treatment with IOX-101 could have resulted in DNA damage, making them to appear in the sub-G_0 region.

Cell invasion and migration of cancer cells in metastasis are considered very important events in cancer progression. We mimicked these situations in the migration assay. IOX-101 remarkably inhibited the migration on A549-CS, indicating the potential of the compound to inhibit cancer cell migration. Metastasis is a complex phenomenon where cells undergo EMT. It was previously shown that tumor stem cells can manifest characteristics of EMT in metastasis[34], which involves biochemical and physiological changes in the cancer cells. During this process, cells express a variety of cytokines and chemokines in their microenvironment[35]. When stimulated by the tumor microenvironment, CSCs can release TNF- , IL-6, and IL-8, which can promote EMT[36]. Inhibition of these key signaling molecules therefore could inhibit metastasis of the CSCs[37]. Dose-dependent inhibition of these cytokine releases from A549-CS further augments the migration inhibitory effects by IOX-101.

Apoptosis is a vital regulatory event that contributes to cell death. Apoptosis could be mediated via either the intrinsic pathway by the mitochondrial cascade that involves Bcl-2/Bax family proteins, active caspases, and Akt signaling or the extrinsic pathway by expressing surface death receptors[38]. In the current study, activation of caspase 3 and caspase 9 by IOX-101 can be interpreted as a biochemical indicator of mitochondria-mediated apoptosis. Increase in the proapoptotic Bax levels and decrease in antiapoptotic Bcl-2 would have attenuated the mitochondrial potential of A549-CS, ultimately making them bioenergetically deficient and undergo apoptosis[39]. It can therefore be inferred that IOX-101 has decreased the Bcl-2/Bax ratio to favor collective apoptosis in A549-CS.

Growing evidence supports the involvement of the Akt/mTOR signaling pathway in chemotherapy-based cancer resistance[40]. Deactivation of this pathway could therefore be an ideal strategy to reverse chemotherapy resistance in cancer cells. In this study, we have shown IOX-101 to reduce activation of Akt and mTOR, which suggests the activity of the compound to be mediated by the Akt/mTOR pathway. Moreover, reversal of MDR-1 and LRP expression in A549-CS by IOX-101 supports the observed efficacy of the compound in the resistant lung cancer model. It is shown that inflammation provokes many cancer types, and one such classical example is lung cancer[41]. NF- B is a vital factor that regulates both inflammatory responses and cell survival[42]. Once activated, NF- B is found to orchestrate a number of cascades, ultimately shutting down the apoptosis and provoking proinflammatory cytokine release to favor metastasis[43]. To further augment our observations on the cytokine release inhibitions by IOX-101, we tested the effect of compound on NF- B-p65 phosphorylation in

A549-CS. Our results demonstrated that IOX-101 could inhibit NF- B activation in A659-CS. As it is established that Akt controls NF- B activation through mTOR, from our observations, we hypothesize that the observed anticancer properties of IOX-101 in A549-CS could have been mediated through the Akt/mTOR/NF- B pathway. However, research on animal models and toxicity studies are needed to demonstrate the in vivo efficacy of the compound and further escalate it to the next phase of drug discovery research.

CONCLUSION

In summary, we conclude that A549-CS could be a robust model for screening drug resistance in an in vitro lung cancer model, where IOX-101 has demonstrable efficacy in CSC-like, sphere-forming cells targeting Akt/mTOR/NF- B signaling proteins. Therefore, IOX-101 has potential promise to be developed as a novel chemotherapeutic against drug-resistant lung carcinoma.

ACKNOWLEDGMENTS: This study was funded by The Deanship of Scientific Research, King Khalid University, Abha, KSA (Approved Project Number G.R.P/448/1439). The authors declare no conflicts of interest.

REFERENCES

1. Housman G, Byler S, Heerboth S. Drug resistance in cancer: An overview. Cancers 2014;6(3):1769–92.
2. Stavrovskaya AA. Cellular mechanisms of multidrug resistance of tumor cells. Biochemistry 2000;65(1):95–106.
3. Holohan C, Van Schaeybroeck S, Longley DB, Johnston PG. Cancer drug resistance: An evolving paradigm. Nat Rev Cancer 2013;13(10):714–26.
4. Chang G, Roth CB. Structure of MsbA from E. coli: A homolog of the multidrug resistance ATP binding cassette (ABC) transporters. Science 2001;293(5536):1793–800.
5. Bonanno L, Favaretto A, Rosell R. Platinum drugs and DNA repair mechanisms in lung cancer. Anticancer Res. 2014;34(1):493–501.
6. Du B, Shim JS. Targeting epithelial–mesenchymal transition (EMT) to overcome drug resistance in cancer. Molecules 2016;22:21–7.
7. Baker EK, El-Osta A. The rise of DNA methylation and the importance of chromatin on multidrug resistance in cancer. Exp Cell Res. 2003;290(2):177–94.
8. Parkin DM, Bray F, Ferlay J, Pisani P. Global cancer statistics, 2002. CA Cancer J Clin. 2005;55:74–108.
9. Dasari S, Tchounwou PB. Cisplatin in cancer therapy: Molecular mechanisms of action. Eur J Pharmacol. 2014;5:364–78.
10. Sarin N, Engel F, Kalayda GV. Cisplatin resistance in non-small cell lung cancer cells is associated with an abrogation of cisplatin-induced G_2/M cell cycle arrest. PLoS One 2017;12(7):e0181081.
11. Schiller JH, Harrington D, Belani CP, Langer C, Sandler A, Krook J, Zhu J, Johnson DH. Comparison of four chemotherapy regimens for advanced non-small-cell lung cancer. N Engl J Med. 2002;346:92–8.
12. Rajagopalan P, Raju M, Aseeri H, Helal IM, Elbessoumy AA. IOX-101, a novel small molecule, reduces AML cell proliferation by Akt enzyme inhibition. Arch Biol Sci. 2018;70(2):321–7.
13. Feng-Feng S, Yong-He H, Lv-Ping X, Xiao-Yun T, Ji-Hua Z, Sheng-Song C, Juan S, Xiao-Qun Y. Enhanced expression of stem cell markers and drug resistance in sphere-forming non-small cell lung cancer cells. Int J Clin Exp Pathol. 2015;8(6):6287–300.
14. Mosmann T. Rapid colorimetric assay for cellular growth and survival: Application to proliferation and cytotoxicity assays. J Immunol. Methods 1983;65:55–63.
15. Maguire O, Loughlin K, Minderman H. Simultaneous assessment of NF- B/p65 phosphorylation and nuclear localization using imaging flow cytometry. J Immunol Methods 2015;423:3–11.
16. Kars MD, Iseri OD, Gündüz U, Ural AU, Arpaci F, Molnár J. Development of rational in vitro models for drug resistance in breast cancer and modulation of MDR by selected compounds. Anticancer Res. 2006;26(6B):4559–68.
17. McDermott M, Eustace AJ, Busschots S, Breen L, Crown J, Clynes M, O'Donovan N, Stordal B. In vitro development of chemotherapy and targeted therapy drug-resistant cancer cell lines: A practical guide with case studies. Front Oncol. 2014;6:40–7.
18. Visvader JE, Lindeman GJ. Cancer stem cells in solid tumours: Accumulating evidence and unresolved questions. Nat Rev Cancer 2008;8:755–68.
19. Fuchs D, Daniel V, Sadeghi M, Opelz G, Naujokat C. Salinomycin overcomes ABC transporter-mediated multidrug and apoptosis resistance in human leukemia stem cell-like KG-1a cells. Biochem Biophys Res Commun. 2010;394:1098–104.
20. Xu XL, Xing BC, Han HB, Zhao W, Hu MH, Xu ZL, Li JY, Xie Y, Gu J, Wang Y, Zhang ZQ. The properties of tumor-initiating cells from a hepatocellular carcinoma patient's primary and recurrent tumor. Carcinogenesis 2010;31:167–74.
21. Liu T, Xu F, Du X, Lai D, Zhao Y, Huang Q, Jiang L, Huang W, Cheng W, Liu Z. Establishment and characterization of multi-drug resistant, prostate carcinoma-initiating stem-like cells from human prostate cancer cell lines 22RV1. Mol Cell Biochem. 2010;340:265–73.
22. Zheng X, Cui D, Xu S, Brabant G, Derwahl M. Doxorubicin fails to eradicate cancer stem cells derived from anaplastic thyroid carcinoma cells: Characterization of resistant cells. Int J Oncol. 2010;37:307–15.
23. Saigusa S, Tanaka K, Toiyama Y, Yokoe T, Okugawa Y, Kawamoto A, Yasuda H, Morimoto Y, Fujikawa H, Inoue Y, Miki C, Kusunoki M. Immunohistochemical features of CD133 expression: Association with resistance to chemoradiotherapy in rectal cancer. Oncol Rep. 2010;24:345–50.
24. Sun FF, Hu YH, Xiong LP, Tu XY, Zhao JH, Chen SS, Song J, Ye XQ. Enhanced expression of stem cell markers and drug resistance in sphere-forming non-small cell lung cancer cells. Int J Clin Exp Pathol. 2015;8(6):6287–300.
25. Wu Y, Wu PY. CD133 as a marker for cancer stem cells: Progresses and concerns. Stem Cells Dev. 2009;(8):1127–34.
26. Luan YZ, Li L, Li DR, Zhang W, Tang BJ. [Establishment of 5 resistant ovarian cancer cell strains and expression of resistance-related genes]. Zhonghua Fu Chan Ke Za Zhi 2004;39(6):403–7.
27. Hu L, McArthur C, Jaffe RB. Ovarian cancer stem-like side-population cells are tumourigenic and chemoresistant. Br J Cancer 2010;102:1276–83.
28. Gangemi R, Paleari L, Orengo AM, Cesario A, Chessa L, Ferrini S, Russo P. Cancer stem cells: A new paradigm

for understanding tumor growth and progression and drug resistance. Curr Med Chem. 2009;16:1688–703.
29. Feng F, Wang B, Sun X, Zhu Y, Tang H, Nan G, Wang L, Wu B, Huhe M, Liu S, Diao T, Hou R, Zhang Y, Zhang Z. Metuzumab enhanced chemosensitivity and apoptosis in non-small cell lung carcinoma. Cancer Biol Ther. 2017;18(1):51–62.
30. Harper LJ, Costea DE, Gammon L, Fazil B, Biddle A, Mackenzie IC. Normal and malignant epithelial cells with stem-like properties have an extended G2 cell cycle phase that is associated with apoptotic resistance. BMC Cancer 2010;10:166.
31. Engeland M, Ramaekers FC, Schutte B, Reutelingsperger CP. A novel assay to measure loss of plasma membrane asymmetry during apoptosis of adherent cells in culture. Cytometry 1996;24:131–9.
32. Nouri K, Yazdanparast R. Proliferation inhibition, cell cycle arrest and apoptosis induced in HL-60 cells by a natural diterpene ester from Daphne mucronata. Daru 2011;19(2):145–53.
33. Sorenson CM., Eastman A. Influence of cis-diammine dichloro platinum (II) on DNA synthesis and cell cycle progression in excision repair proficient and deficient Chinese hamster ovary cells. Cancer Res. 1988;48:6703–7.
34. Hsiao YJ, Su KY, Hsu YC, Chang GC, Chen JS, Chen HY, Hong QS, Hsu SC, Kang PH, Hsu CY. SPANXA suppresses EMT by inhibiting c-JUN/SNAI2 signaling in lung adenocarcinoma. Oncotarget 2016;7:44417–29.
35. Shang Y, Cai X, Fan D. Roles of epithelial–mesenchymal transition in cancer drug resistance. Curr Cancer Drug Targets 2013;13(9):915–29.
36. Rhee KJ, Lee JI, YW. Mesenchymal stem cell-mediated effects of tumor support or suppression. Int J Mol Sci. 2015;16:30015–33.
37. Ge A, Ma Y, Liu YN, Li YS, Gu H, Zhang JX, Wang QX, Zeng XN, Huang M. Diosmetin prevents TGF- 1-induced epithelial mesenchymal transition via ROS/MAPK signaling pathways. Life Sci. 2016;153:1–8.
38. Zhang BG, Du T, Zang MD, Chang Q, Fan ZY, Li JF, Yu BQ, Su LP, Li C, Yan C, Gu QL, Zhu ZG, Yan M, Liu B. Androgen receptor promotes gastric cancer cell migration and invasion via AKT-phosphorylation dependent upregulation of matrix metalloproteinase 9. Oncotarget 2014;5(21):10584–95.
39. Wong BS, Hsiao YC, Lin TW, Chen KS, Chen PN, Kuo WH, Chu SC, Hsieh YS. The in vitro in vivo apoptotic effects of Mahoniaoiwakensis on human lung cancer cells. Chem Biol Interact. 2009;180(2):165–74.
40. Liu M, Qi Z, Liu B. RY-2f, an isoflavone analog, overcomes cisplatin resistance to inhibit ovarian tumorigenesis via targeting the PI3K/AKT/mTOR signaling pathway. Oncotarget 2015;6:25281–94.
41. Karin M, Lawrence T, Nizet V. Innate immunity gone awry: Linking microbial infections to chronic inflammation and cancer. Cell 2006;124(4):823–35.
42. DiDonato JA, Mercurio F, Karin M. NF-kappaB and the link between inflammation and cancer. Immunol Rev. 2012;246:379–400.
43. Greten FR, Eckmann L, Greten TF, Park JM, Li ZW, Egan LJ. IKKbeta links inflammation and tumorigenesis in a mouse model of colitis-associated cancer. Cell 2004;118:285–96.